Estimation of phase and group velocities for multi-modal ground roll using the 'phase shift' and 'slant stack generalized S transform based' methods

Roohollah Askari, Robert J. Ferguson, Kristof DeMeersman

ABSTRACT

Phase and group velocities are two important factors that determine shear wave velocity in Multi-channel Analysis of Surface Wave (MASW) surveys. In this study, we present two different methods. The phase shift method and the slant stack generalized S transform based method for the estimation of the phase and group velocities respectively. The phase shift method uses the idea of the slant stack in the Fourier domain to estimate the phase velocity. The slant stack generalized S transform based method uses the slant stack idea in the time-frequency domain based on the generalized S transform. These methods are robust to estimate phase and group velocities where ground roll is multi-modal. We anticipate that, through inversion of the phase and group velocities of multi-modal ground rolls, a better estimation of near surface shear wave velocity will be obtainable.

INTRODUCTION

One of the most important goals in engineering studies is the estimation of soil rigidity for the near surface (Xia et al., 2002a). Due to the dependency of soil rigidity and shear wave velocity, accurate estimation of shear wave velocity is a key factor in engineering studies. Although, seismic refraction methods are one of the conventional methods used for shear wave velocity estimation (Palmer, 1980), they fail to estimate S-velocity where geological structure is complex (Xia et al., 2002b) or where hidden layers (a layer whose velocity is less than its upper layer) are present (Sheriff and Geldart, 1986).

As an alternative to the refraction methods, the analysis of dispersed surface waves (Rayleigh and Love waves) is a well-known procedure to estimate shear wave velocity (e.g. Evison et al., 1959; Stokoe et al., 1988; Keilis- Borok, 1989; Lay and Wallace, 1995; Xia et al., 1999). The method is a based on the inversion of a surface wave dispersion curve (either phase or group velocity curves) calculated from a real data to a vertical shear wave velocity profile. Some studies indicate that the method overcomes the pitfalls of the refraction methods such as geological complexity (Xia et al., 2002b) or the presence of hidden layers (Feng et al., 2005).

Since surface wave methods are based on the inversion of phase and group velocities to a shear wave velocity profile, the processing of data in order to truly estimate a dispersion curve is very crucial. Many algorithms have been developed to address this issue in different transform domains such as FK transform (Yilmaz, 1987), ω-p transform (McMechan and Yedlin, 1981), the wavelet transform (Kulesh et al., 2005; Holschneider et al., 2005; Kulesh et all, 2008) and the generalized S transform (Askari and Ferguson; 2011) for phase velocity, and narrow band-pass filtering (Herrmann, 1973), the wavelet transform (Kulesh et al., 2005; Holschneider et al., 2005) and the generalized S transform (Askari and Ferguson, 2011) for group velocity.

Multi-channel Analysis of Surface Waves (MASW) is a surface wave method based on multi-channel seismic recorded ground roll for near surface studies (Park, 1999). In this study, we present two methods for the estimation of the phase and group velocities for the MASW survey respectively. The phase shift (Park et al., 1998) is a method which is based on the estimation of the Fourier phase spectrum difference from one trace to another for the estimation of the phase velocity. Then, we introduce a slant stack model based on the generalized S transform (Pinnegar and Mansinha, 2003) to estimate the group velocity of multi-channel ground roll.

PHASE SHIFT METHOD

Considering a seismic record in the time-offset domain u(t,x) containing the ground roll, the Fourier transform for each trace is expressed

$$U(x,\omega) = \int u(x,t)e^{-i\omega t}\,dt. \tag{1}$$

The equation above could be rewritten as

$$U(x,\omega)=P(x,\omega)A(x,\omega), \tag{2}$$

where P(x,ω) is the phase spectrum and A(x,ω) is the amplitude spectrum. The amplitude spectrum contains all the information about attenuation and spherical divergence whereas the phase spectrum contains all the information about dispersion. Applying the operator $e^{i2\pi fx/v_p}$ where v_p is a phase velocity to the following integral

$$V(f,v_p) = \int \frac{U(x,\omega)}{|U(x,\omega)|} e^{i2\pi fx/v_p} dx = \int P(x,\omega) e^{i2\pi fx/v_p} dx, \tag{3}$$

we obtain a two dimensional image of the phase velocities versus frequencies (Park et al., 1998). It is clear that at those frequencies where v_p is equal to the phase velocities of the signal, the integral will have a maximum. Figure 1 shows synthetic data containing a two modal ground roll. The geophone spacing is one meter and the sampling is 2ms. The initial wavelets that are used in the both modes are a Ricker wavelet. Figure 2 shows the phase velocity obtained from the phase shift method. The solid and dashed lines correspond to the theoretical phase velocities. As seen, the theoretical values are well matched to the estimated. Figure 3 shows a real shot record. The sampling interval is 10m and the sampling frequency is 500Hz. Figure 4 is the phase velocity obtained from the phase shift method. As seen the fundamental mode phase velocity from 400m/s to 200m/s is clearly observable for the frequency ranges from 4Hz to 12Hz and a higher mode phase velocity from 450m/s to 350m/s could be observable for the frequency ranges from 12Hz to 20Hz.

THE GENERALIZED S-TRANSFORM

The S transform is a time-frequency transform which provides a time depended frequency distribution of a signal. The idea presented in the S transform is very similar to that in the Gabor transform (Gabor, 1946) which utilizes a Gaussian window for spectral localization. But, in the S transform, the Gaussian window is scalable with the frequency which enhances a better time-frequency resolution. The S transform is given by Stockwell et al. (1996) as

$$S[h(\tau)](t,f) = \int_{-\infty}^{+\infty} h(\tau)\left[\frac{|f|}{\sqrt{2\pi}} e^{-\frac{f^2(\tau-t)^2}{2}}\right] e^{-j2\pi f\tau} d\tau. \tag{4}$$

where as an operator S transforms h into a function of frequency f and time t. Time t controls the position of the Gaussian window on the output time axis.

In practice, it is possible to insert a multi-parameter factor **p** in the Gaussian window of the S transform in order to manipulate the time-frequency resolution of the S transform based on our processing or interpretational purposes. Therefore the idea of the generalized S transform is introduced. The generalized S transform is

$$S_g[h(\tau)](t,f,\mathbf{p}) = \int_{-\infty}^{+\infty} h(\tau) w(\tau - t, f, \mathbf{p}) e^{-j2\pi f\tau} d\tau, \tag{5}$$

where the Gaussian window of the S transform is generalized into the modeling window *w* whose width and shape are now a function of parameter **p**. A version of the generalized S transform that has particular usefulness in our analysis is defined using

$$w(\tau - t, f, \mathbf{p}) = \frac{|f|}{\sqrt{2\pi}\sigma} e^{-\frac{f^2(\tau-t)^2}{2\sigma^2}}, \tag{6}$$

where, compared with the Gaussian window in equation (4), a scaling factor σ is introduced (Pinnegar and Mansinha, 2003). Using σ, the generalized S transform is written

$$S_g[h(\tau)](t,f,\sigma) = \int_{-\infty}^{+\infty} h(\tau) \frac{|f|}{\sqrt{2\pi}\sigma} e^{-\frac{f^2(\tau-t)^2}{2\sigma^2}} e^{-j2\pi f\tau} d\tau, \tag{7}$$

where the scaling factor σ controls time-frequency resolution by changing the number of oscillations within the window. We use this version of the generalized S transform in this paper. If we choose a small values of the scaling factor ($\sigma \cong 1$), the generalized S transform presents a better time resolution and a low frequency resolution. On the other hand, choosing a larger value of the scaling factor ($\sigma \gg 1$) results a better frequency resolution in the cost of the time resolution (Askari and Ferguson, 2011). This properly of the generalized S transform can be applied in the slant stack generalized S transform method to improve the estimation of the group velocity at different frequencies.

THE WAVE PROPAGATION OPERATOR

Assuming geometrical spreading correction has been applied on surface wave data, if $h_1(\tau)$ is the wavelet at station 1, the wavelet $h_2(\tau)$ recorded at station 2 can be expressed

$$H_2(f) = e^{-\lambda(f)d} e^{-j2\pi k(f)d} H_1(f), \tag{10}$$

where λ(f) is an attenuation function, and k(f) is a spatial wavenumber that controls wave propagation from station 1 to station 2. This wavenumber characterizes horizontal propagation of surface wave and is a function of elastic properties of the medium, and d is the distance between, the two stations.

Askari and Ferguson (2011) assume that attenuation function λ(f) and phase function k(f) vary slowly with respect to the effective size of the spectrum of the generalized S transform. For instance, for fixed point (t, f) on the time-frequency plane, we may develop λ and k around the central frequency f. Assuming, the wavenumber term k(f) on the right-hand side of equation (10) behaves linearly in the vicinity of f and attenuation function λ(f) is constant in that vicinity where the vicinity is defined by the width of the Gaussian window. Therefore, λ(f+α) and k(f+α) can be expressed

$$\lambda(f+\alpha) = \lambda(f) + O(\alpha), \tag{12}$$

and

$$k(f+\alpha) = k(f) + \alpha k'(f) + O(\alpha^2), \tag{13}$$

where k'(f) indicates a frequency derivative of k(f). Using the above approximations, the generalized S transform of the wavelet is station 2 can be linked to that in station 1 with the following equation (Askari and Ferguson, 2011)

$$S_g[h_2(\tau)] = e^{-j2\pi fd/v_p(f)} e^{-\lambda(f)d} S_g[h_1(\tau)]\big(t - d/v_g(f), f\big) \tag{14}$$

where $S_g[h_1(\tau)]\big(t - d/v_g(f), f\big)$ is the generalized S transform of h_1 shifted by - $d/v_g(f)$ and v_g is the group velocity which is the velocity of a wave pocket (envelope) of surface wave around frequency f.

Based on equation (14), any point at time-frequency plane (t, f) of station 1, is equivalent to the time shifted-frequency plane (t-$d/v_g(f)$, f) of station 2 whose phase difference is $-j2\pi fd/v_p(f)$, and whose amplitude is proportional to $e^{-\lambda(f)d}$ that of station 1. Thus, the group velocity can be obtained from the time difference of the ridge of the transforms for any frequency. Figures 5a and 5b show two synthetic traces of two stations and Figure 5c and Figure 5d show their amplitude spectra respectively. At the first step, ridges of the amplitude spectra of the transform are found (Figures 5c and 5d) at any specific frequency (here f =150Hz) with respect to the time axis. Thus the group velocity is obtained as

$$v_g = d/\Delta t, \tag{15}$$

where $\Delta t = t_2 - t_1$ is the time difference between two ridges. In the real world, a seismic record is composed of multi-modal ground roll therefore the estimation of the group velocity is not as straightforward as equation (15). Therefore in order to adjust the method for a real case, the slant stack generalized S transform based is introduced.

SLANT STACK GENERALIZED S TRANSFORM BASED

The plane wave of a wavefield such as a common shot gather can be transform from the offset-time domain to the intercept time-slowness domain. This transformation is achieved by applying linear moveout and summing amplitudes over the offset axis. This procedure is called slant stack (Yilmaz, 1987). The first step which is a linear moveout is expressed as

$$U(x, T) = U(x, T = t - px), \tag{16}$$

where T is intercept time and p is slowness. The second step which is the staking of all the amplitude over the offset with respect to their slownesses and intercept times is expressed as

$$\mathrm{P}(\mathrm{p},\mathrm{T}) = \sum_{\mathrm{x}} \mathrm{U}(\mathrm{x}, \mathrm{T} = \mathrm{t} - \mathrm{px}), \tag{17}$$

where P is the slant stack function. Therefore it is possible to find the slownesses of linear phenomena on a seismic record using slant stack idea. Combining the idea represented by equation (14) with that in equation (17), we can provide the group velocity of multi-modal ground roll. In this study we call this approach the slant stack generalized S transform based.

Considering the synthetic data represented in Figure 1, the generalized S transform is calculated for each trace (Figure 6a). For any specific frequency such as 40Hz in the generalized S transform domain, there is a pseudo-seismic trace which is a function of time (Figure 6b). Putting together all of the pseudo-traces for different offsets, we make a pseudo-seismic record for that frequency (Figure 7). According to the linear propagation of ground roll on surface, the apparent velocity of the ground roll can be estimated by applying the slant stack transformation. Figure 8a shows the slant stack of the pseudo-seismic record in Figure 7. We show the slant stack in the intercept-time-velocity domain instead of the intercept-time-slowness domain for giving a better understanding of the velocity ranges of the group velocity. As seen, at T=0 (Figure 8b), we can estimate the group velocity for that frequency. Therefore, we can make a 2D image of the group velocity of the ground roll by putting together all the velocities estimated at intercept time T=0, for all frequencies. Figure 9 shows the group velocity of the record in Figure 1 based on the scaling factor σ=1. As seen, the group velocity is well estimated for frequencies smaller than 90Hz. However the estimated group velocity for frequencies larger than 90Hz is overestimated. This can be explained due to the frequency uncertainty of the generalized S transform at higher frequencies. In order to better estimate group velocity for higher frequencies, a larger scaling factor should be chosen. Figure 10 shows the group velocity based on the scaling factor σ=5. In this case, the group velocity is better estimated comparatively with the case σ=1. However at low frequencies especially for frequencies below 50 Hz, the group velocity resolution is weakened due to the low time resolution of the generalized S transform for low frequencies for larger scaling factor. Figure 11 shows the group velocity based on the scaling factor σ=20. The estimated group velocity is better estimated compared to that of the scaling factor σ=1 and σ=5, but, for low frequencies, the resolution is more weakened. Therefore there is a tradeoff between the group velocity resolution of low frequencies when a small scaling factor is chosen and that of high frequencies when a large scaling factor is chosen. Based on our imperial observations, scaling factors 1 to 5 give reasonable results for the ranges of frequencies (5-100Hz) in the MASW survey. We have applied the slant stack generalized S transform on the real data in Figure 3 to estimate the group velocity. Figure 12 shows the group velocity. The estimated group velocity is less than the estimated phase velocity which is well consistent with other observations (e.g. Kulesh et al., 2005; Holschneider et al., 2005; Askari and Ferguson, 2011). The ranges of the group velocity vary from 100m/s at frequency 18Hz to 400m/s at frequency 3Hz. These rages of the group velocity are also consistent with the group velocity of ground roll for near surface.

CONCLUSION

In this study we present two different methods for the estimation of the phase and group velocities respectively. The phase shift method is fast and high resolution that can be used for the estimation of multi-modal ground roll. The resolution of the phase velocity can be improved by zero padding.

We also introduce the slant stack generalized S transform based for the estimation of the group velocity. As we show in this paper, the resolution of the group velocity is manipulated by a scaling factor. As smaller scaling factor should be chosen for the low frequency ground roll. However, for higher frequencies, a larger scaling factor should be chosen. Therefore, there is a trade of between the resolution of low and high frequency ground roll. Based on our imperial observations, for the ranges of the frequencies that we deal with in the MASW survey (3-100Hz), scaling factors from 1 to 5 are recommended.

ACKNOWLEDGEMENTS

The authors wish to express our gratitude to CGGVeritas for providing facilities to do this research. We thank to us the sponsors, faculty, and staff of the Consortium for Research in Elastic Wave Exploration Seismology (CREWES), as well as the Natural Sciences and Engineering Research Council of Canada (NSERC, CRDPJ 379744-08), for their support of this work. We also thank to Petrobank for proving us with the real data.

REFERENCES

Askari, R., and Ferguson, R. J., 2011, Dispersion and the dissipative characteristics of surface waves in the generalized S transform domain: Geophysics, in press.

Evison, F. F., Orr, R. H., and, Ingham, C. E., 1959, Thickness of the earth's crust in Antarctica: Nature, 183, 306-308.

Feng, S., Sugiyama,T., and Yamanaka, H., 2005, Effectiveness of multi-mode surface wave inversion in shallow engineering site investigations: Exploration Geophysics, 36, 26-33.

Gabor, D., 1946, Theory of communication: J. Inst. Elect. Eng., 93, 429–457.

Herrmann, R. B., 1973, Some aspects of band-pass filtering of surface waves: Bull. seism. Soc. Am, 63, 663–671.

Holschneider, M., Diallo, M. S., Kulesh, M., Ohrnberger, M., Lu ̈ck, E., and Scherbaum, F., 2005, Characterization of dispersive surface waves using continuous wavelet transforms: Geophys. J. Int., 163, 463–478.

Keilis-Borok, V. I., 1989, Seismic Surface Waves in Laterally Inhomogeneous Earth: Kluwer Academic Publishers, London.

Kulesh, M., Holschneider, M., Diallo, M. S., Xie, Q., and Scherbaum, F., 2005, Modeling of wave dispersion using continuous wavelet transforms: Pure and Applied Geophysics, 162, 843–855.

Kulesh, M., Holschneider, M., Ohrnberger, M., and Lu ̈ck. E., 2008, Modeling of wave dispersion using continuous wavelet transforms II: wavelet-based frequency-velocity analysis: Pure and Applied Geophysics, 165, 255–270.

Lay, T., and Wallace, T. C., 1995, Modern Global Seismology: Academic Press, London, UK.

McMechan, G., and Yedlin, J. M., 1981, Analysis of dispersive waves by wave field transformation: Geophysics, 46, 869-874.

Palmer, D., 1980, The generalized reciprocal method of seismic refraction interpretation: Society of Exploration Geophysicists, Tulsa, OK, 104 p.

Park, C. B., Miller, R. D. and Xia, J., 1998, Imaging dispersion curves of surface waves on multi-channel record, Technical Program with Biographies SEG, 68th Annual Meeting, New Orleans, LA., 1377–1380.

Park, C.B., and Miller, R.D., Xia, J., 1999, Multichannel analysis of surface waves: Geophysics, 64, 800–808.

Pinnegar, C. R., and Mansinha, L. 2003, The Bi-Gaussian S-transform: SIAM J. SCI. COMPUT., 24, 1678–1692.

Sheriff, R.E., and Geldart, L.P., 1986, Exploration Seismology, Vol. 12. Cambridge University Press, Cambridge, UK.

Stockwell, R. G., Mansinha, L., and Lowe, R. P., 1996, Localization of the complex spectrum: The S transform: IEEE Transactions on Signal Processing, 44, 998-1001.

Stokoe II, K.H., Nazarian, S., Rix, G.J., Sanchez-Salinero, I., Sheu, J., and Mok, Y., 1988. In situ seismic testing of hard-to-sample soils by surface wave method: Earthquake Engineering and Soil Dynamic. II — Recent adv. in ground-motion eval. ASCE, Park City, pp. 264–277.

Xia, J., Miller, R.D., and Park, C.B., 1999, Estimation of near-surface shear-wave velocity by inversion of Rayleigh waves: Geophysics, 64, 691–700.

Xia, J., Miller, R. D., Park, C. B., Hunter, J. A., Harris, J. B., and Ivanov J, 2002a, Comparing shear wave velocity profiles inverted from multichannel surface wave with borehole measurements: Soil Dynamics and Earthquake Engineering, 22, 181-190.

Xia, J., Miller, R. D., Park, C. B., Wightman, E., and Nigbor, R., 2002b, A pitfall in shallow shear-wave refraction surveying: Journal of Applied Geophysics, 51, 1 – 9.

Yilmaz, O., 1987, Seismic Data Processing: Soc. Exploration Geophysicists, Tulsa, OK.

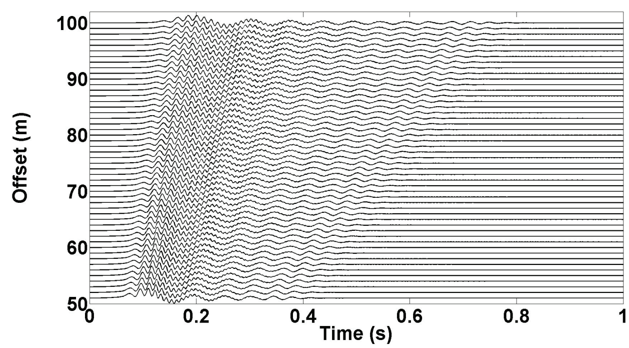

Fig. 1. A synthetic data containing a two modal ground roll.

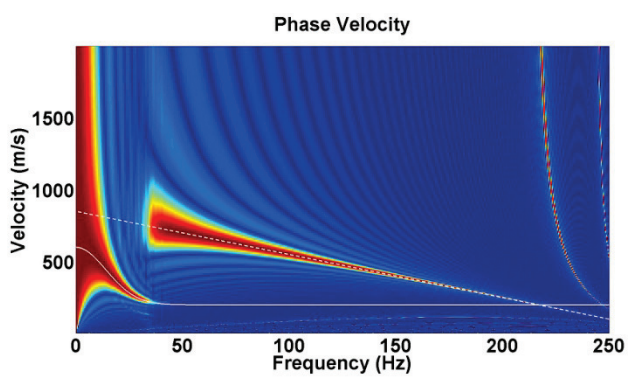

Fig. 2. The phase velocity of the record in Figure 1 obtained from the phase shift method.

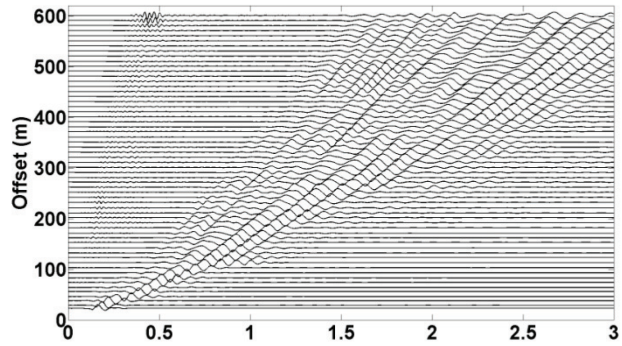

Fig. 3. A real shot record.

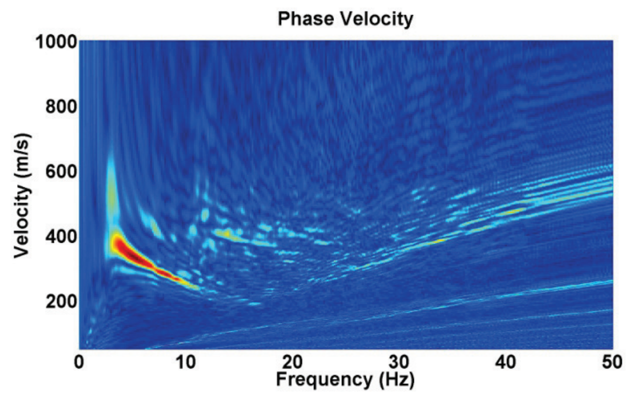

Fig. 4. The phase velocity of the record in Figure 3 obtained from the phase shift method.

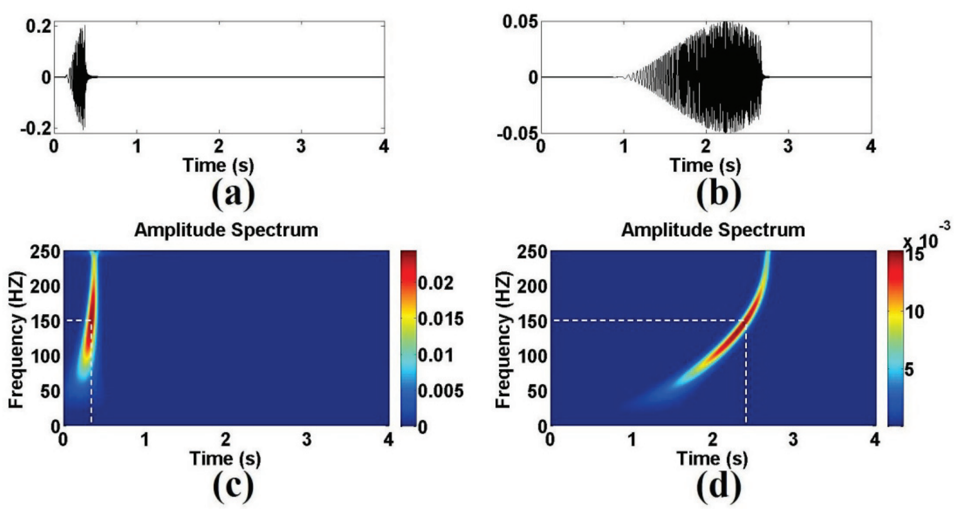

Fig. 5. (a) and (b) two synthetic traces. (c) and (d) the amplitude spectra of the first and second traces respectively.

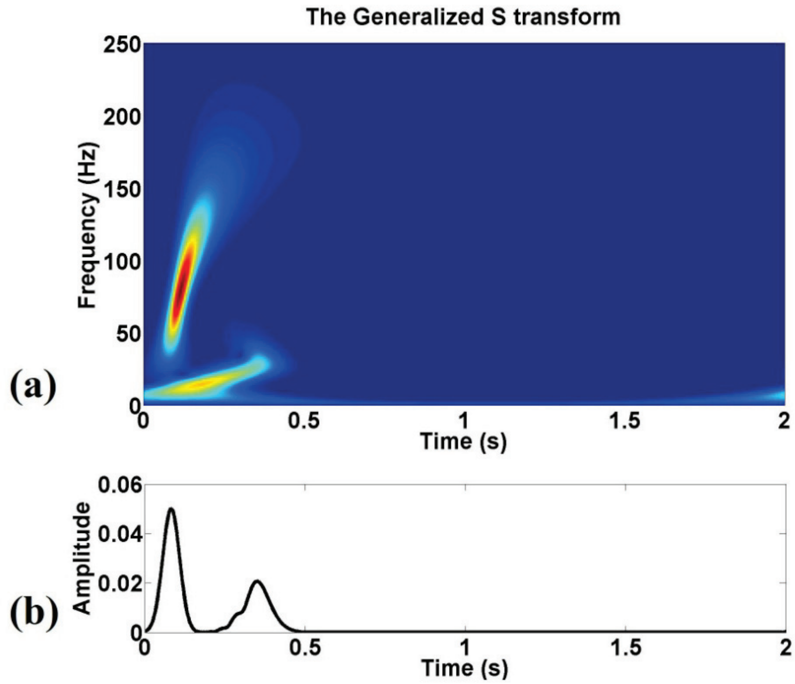

Fig. 6. (a) The generalized S transform of the first trace in Figure 1. (b) Time representation of the generalized S transform at the single frequency 40Hz.

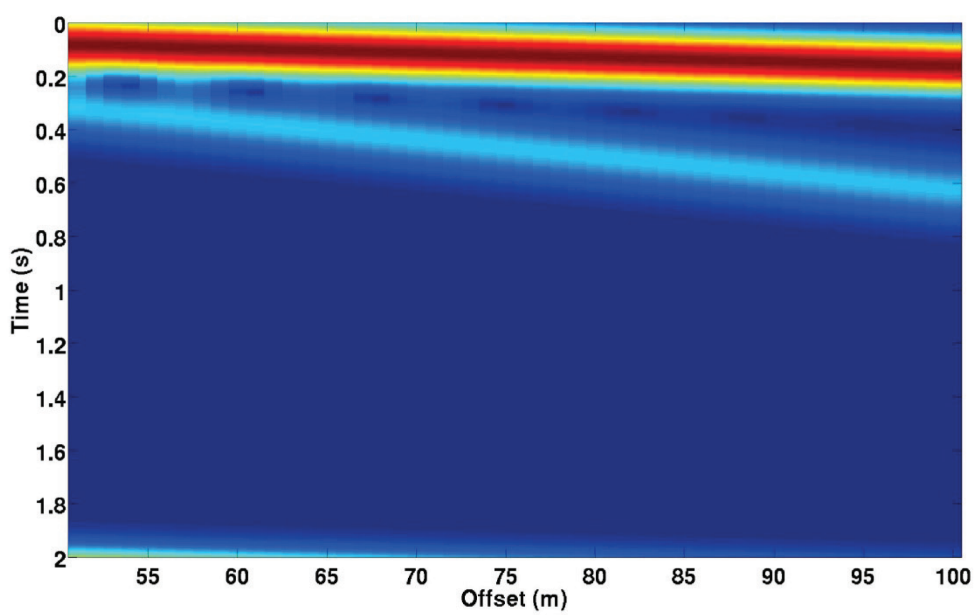

Fig. 7. A pseudo-seismic record based of the generalized S transform of the traces of the record in Figure 1 at Frequency=40Hz.

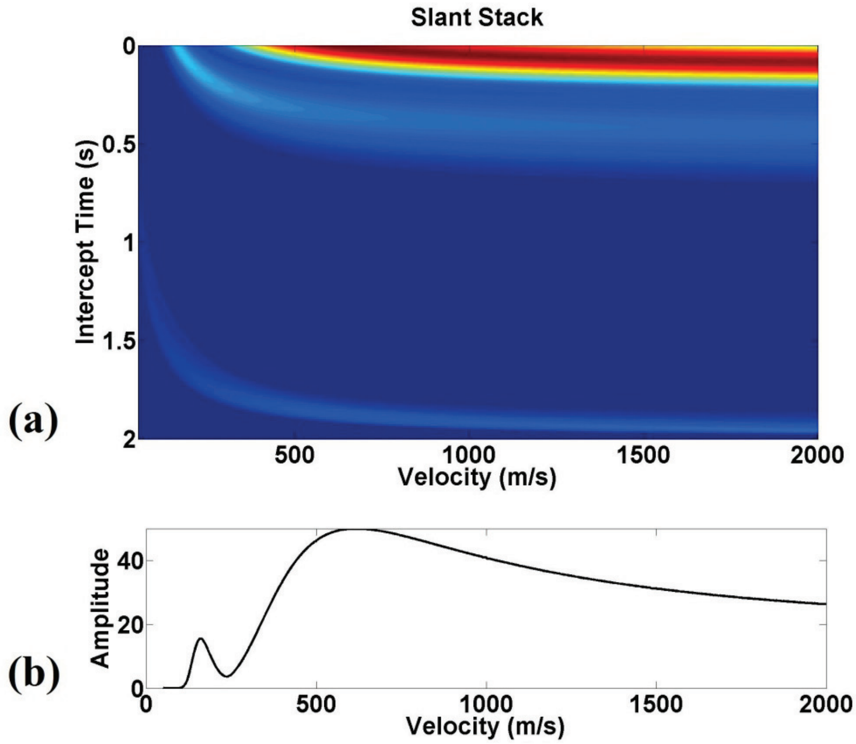

Fig. 8. (a) The slant stack of the pseudo-record in Figure 7. (b) Single representation of the slant stack at intercept time T=0.

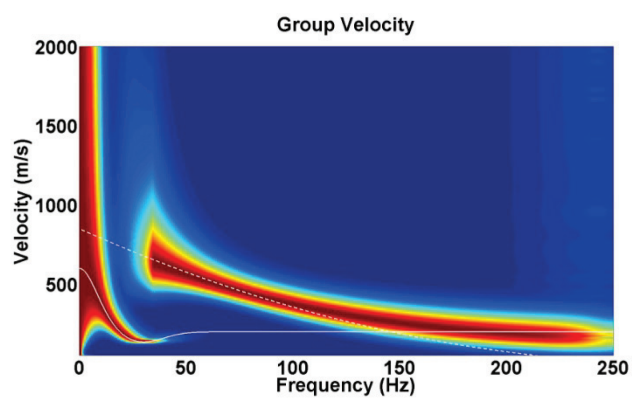

Fig. 9. The estimated group velocity for the record in Figure 1 based on the scaling factor σ=1. The solid and dashed lines correspond to the theoretical values.

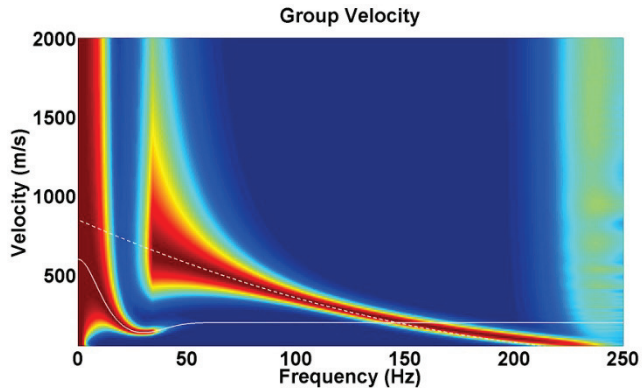

Fig. 10. The estimated group velocity for the record in Figure 1 based on the scaling factor σ=5. The solid and dashed lines correspond to the theoretical values.

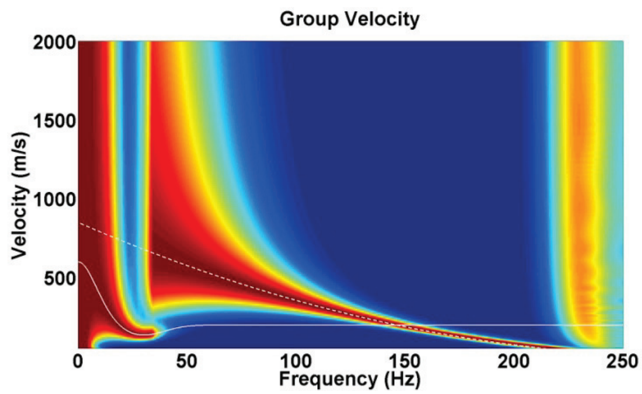

Fig. 11. The estimated group velocity for the record in Figure 1 based on the scaling factor σ=20. The solid and dashed lines correspond to the theoretical values.

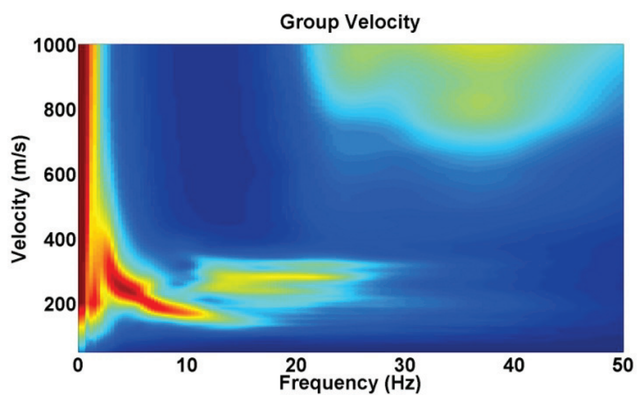

Fig. 12. The estimated group velocity for the record in Figure 3 based on the scaling factor σ=1.